TEVATRON STUDY REPORT: PROTON BEAM LIFETIME AT 150 GEV, CHROMATICITY AND TUNE SCANS, APERTURE, SCRAPING 12/03-04/02

P. Ivanov, P. Lebrun, T. Sen, V. Shiltsev, X.L. Zhang, F. Zimmermann*

Abstract

During a dedicated machine study on December 3-4, 2002, we measured the chromaticities, the proton beam lifetime and loss rates at 150 GeV on the central orbit, the proton helix, and the pbar helix. On the proton helix we dry-fired rhe pbar injection to observe a possible impact of injection kickers and wire scans. We next studied the dependence of the lifetime on tunes and on chromaticity, for both helices. At this occasion, we found an instability threshold for the pbar helix. We reduced the vertical aperture by moving collimator F49VCP closer to the beam, and measured the effect on the loss rate. We lastly removed a part of the proton beam by this collimator to get an emittance estimate independent of the flying wires.

1 SEQUENCE OF EVENTS

At 21:54 we measured tunes and chromaticities using an uncoalesced beam. The chromaticities were Ch=7.3, Cv=8.8 on the central orbit (the closest tune approach was 0.0055), Ch=10.8, Cv=11.7 on the proton helix, and Ch=7.3, Cv=7.3 on the pbar helix. Schottky spectra for all three orbits are shown in Figs. 1-3.

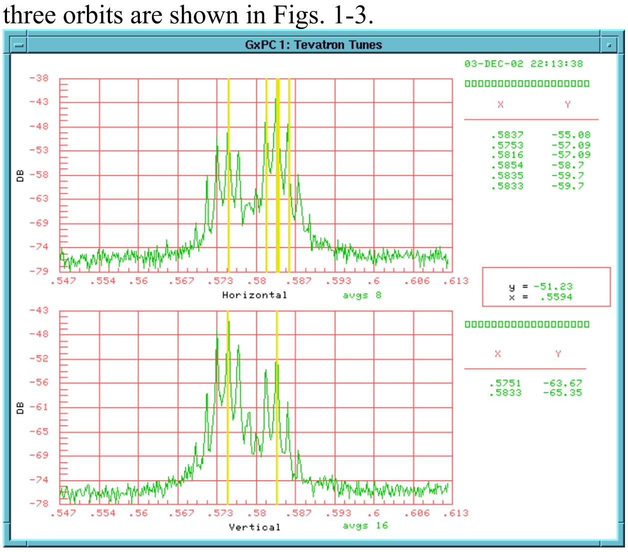

Figure 1: Schottky spectra for uncoalesced beam on the central orbit.

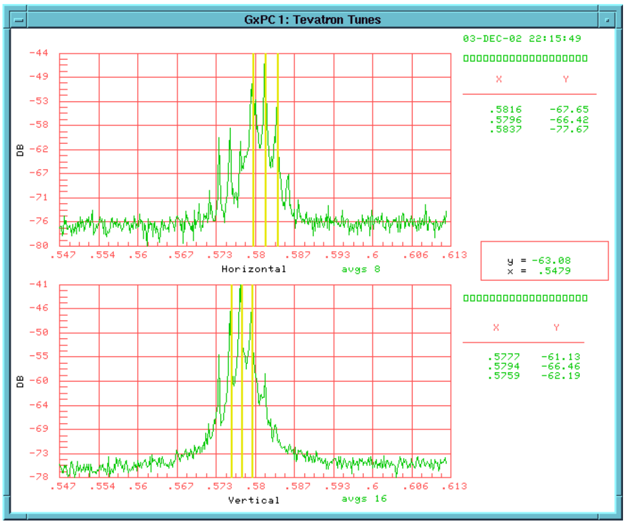

Figure 2: Schottky spectra for uncoalesced beam on the proton helix.

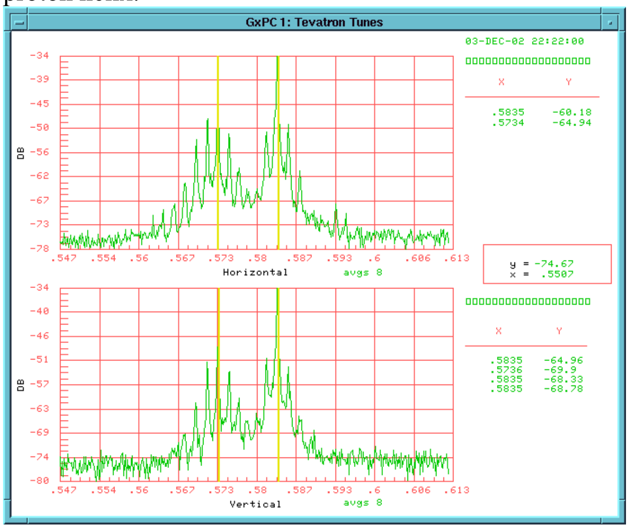

Figure 3: Schottky spectra for uncoalesced beam on the pbar helix.

At 22:30 we injected a train of 12 coalesced proton bunches. The transverse dampers were off. From 22:41 on we stored the beam on the proton helix. Figure 4 shows the flying-wire profile of bunch 1, and Fig. 5 the TevArray display with intensities, bunch lengths, and emittances for all bunches. The beam lifetime deduced from an exponential fit to IBEAM over about 15 minutes was 1.55 hours, the exponential decay time of the bunch length was 3.55 hr.

*visiting from CERN

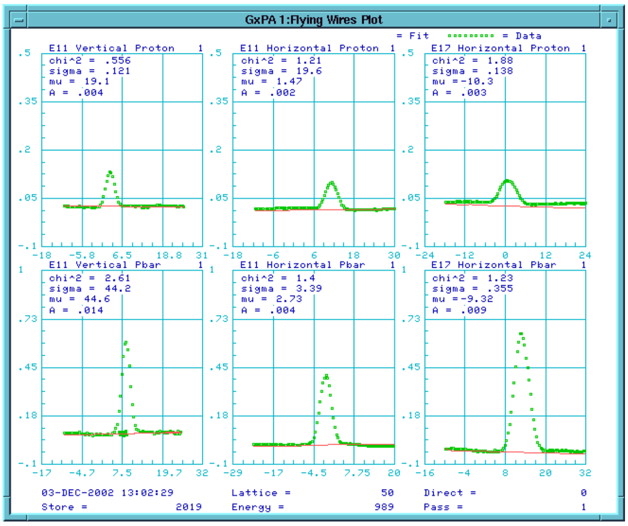

Figure 4: Flying wire profile for proton bunch 1 after storing the beam on the proton helix.

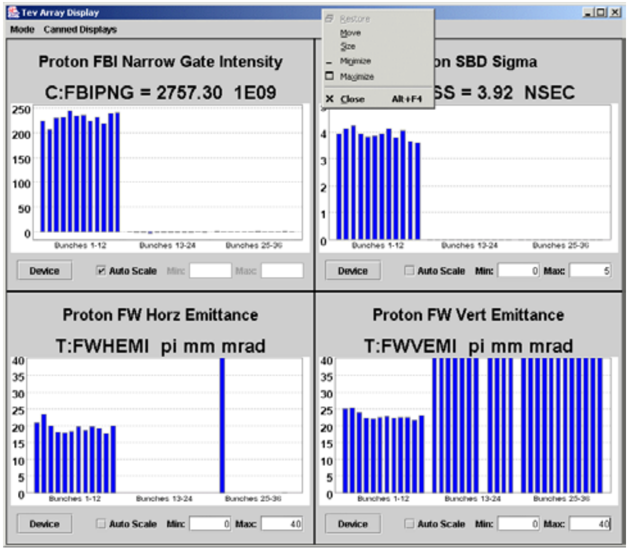

Figure 5: Intensities, rms bunch length, and normalized emittances for all bunches, after storing the beam on the proton helix. Only the first twelve bunches are present; the other data can be ignored.

From 22:55 we dry-fired the pbar injection twice for 9 times. Figure 6 shows a Schottky spectrum recorded during this time, which exhibits a strong peak above a tune of 0.6. From 23:10, the set of 9 dry injections was repeated, since the pbar injection aggregate had not been run, and, thus, the implication of the dry injection was unclear. Prior to the second time the aggregate was executed. Figures 7 and 8 show the emittances measured before and after the 18 times of pbar kicker dry firing. While the vertical emittance is reduced by about 10%, the horizontal emittance increased by 40%. Therefore, the pbar kickers could have a significant effect on the proton-beam emittance. On the other hand, the beam lifetime actually improved during the dry-firing of the pbar injection. The beam lifetime from T:IBEAM fitted over the time interval of the pbar injection dry firing (from 22:55 to 23:22) was 2.2 hrs and the bunch length decay time 7.4 hr.

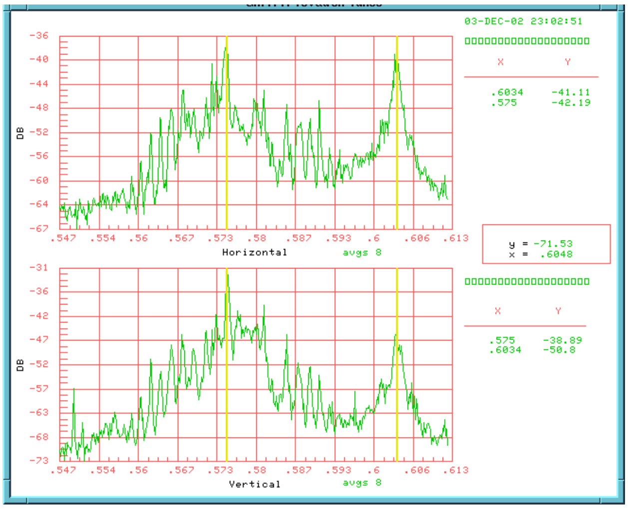

Figure 6: Schottky spectrum recorded at the time of the pbar injection dry firing, revealing a large peak above 0.6.

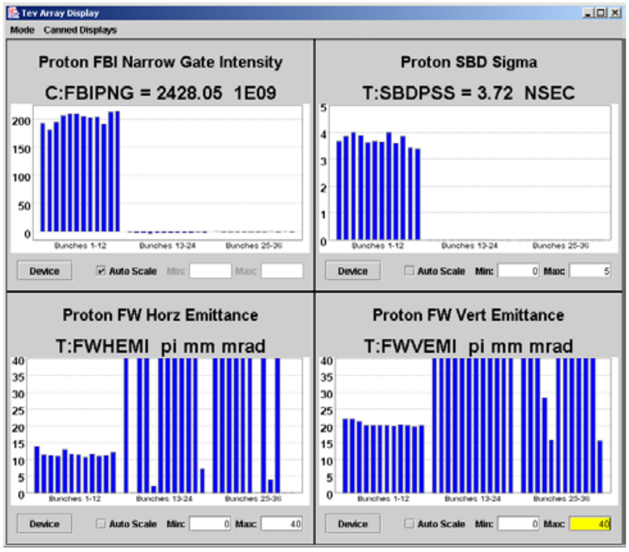

Figure 7: TevArray display with emittances for 12 bunches prior to pbar kicker dry firing Only the first twelve bunches are present; the other data can be ignored..

From 23:30 to 0:20 we scanned the tunes on the proton helix. The initial base injection tunes were 20.61 horizontally and 20.583 vertically. We changed the vertical tune over a range –0.005 to +0.004., and the horizontal from –0.005 to +0.002. The loss rates and Schottky power were sensitive to the horizontal tune, but fairly independent of the vertical. For this reason, we later calibrated the tune knobs (see below). The intensities and emittances after the tune scan are shown in Fig. 9. From

0:20 we next scanned the horizontal and vertical chromaticities. The initial chromaticity settings (on T55 page) were 43 and 30, respectively. From about 1:07 to 1:20 the Tevatron was ramped, to prepare for a new injection. Figures 10 and 11 display the emittances before and after the ramp. In Fig. 10 we see that the horizontal emittance after the chromaticity scan was much smaller than before, presumably due to the beam loss during this scan. Figure 11 illustrates that starting from the small emittance a significant emittance growth by a factor 2-3 occurred on the ramp.

At 3:00 we calibrated the QH & QV tune knobs at injection with uncoalesced protons on the central orbit. At 3:05 we injected a single coalesced proton bunch and this time placed it on the pbar helix. On the pbar helix the exponential beam lifetime fitted over 15 minutes was 2.5 hrs. The SBD bunch-length measurement was not working and we cannot be sure that the proton-bunch had the same parameters as in the previous experiment on the proton-helix. At 3:30 we performed a chromaticity scan on the pbar helix. Initial base chromaticity settings were 42 and 32. We found an instability threshold at a vertical chromaticity setting of 29 (–3 units lower than the starting point), where we lost a significant portion of the beam.

At 3:46 a fresh proton bunch was injected on the central orbit. From 4:07 we performed a scraping study for a single bunch on the central orbit using the vertical collimator F49VCP, in order to measure the loss rate and the lifetime as a function of aperture. Figure 12 shows the beam size of this bunch prior to the scraping as recorded by the flying wires. The collimator position, intensity decrease, and loss rates during the scraping are illustrated in Fig. 13.

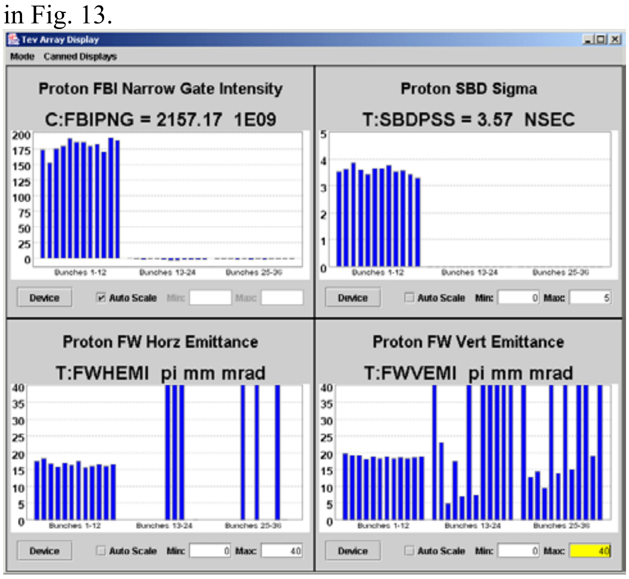

Figure 8: TevArray display with emittances for 12 bunches after 18 times of pbar kicker dry firing.

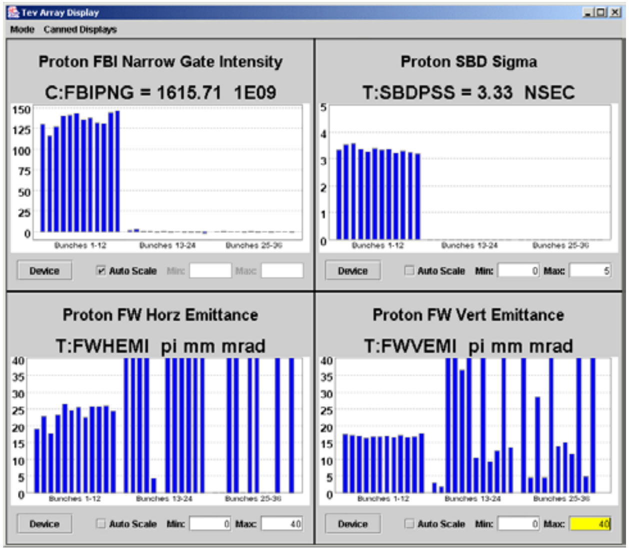

Figure 9: TevArray display with emittances for 12 bunches after the tune scan on the proton helix.

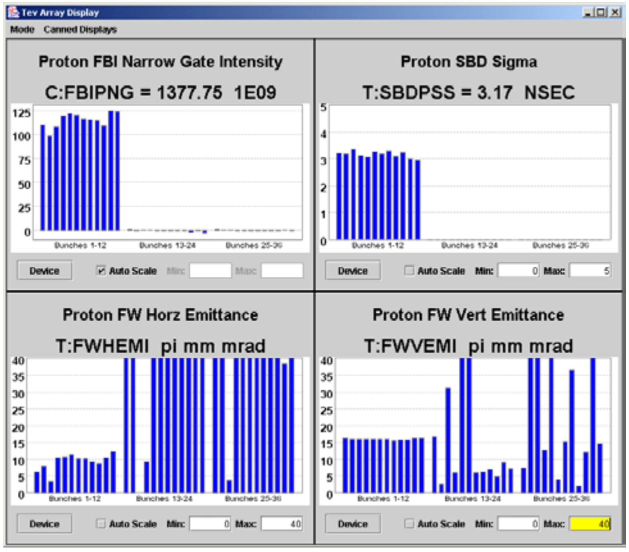

Figure 10: TevArray display with emittances for 12 bunches before the ramp on the proton helix.

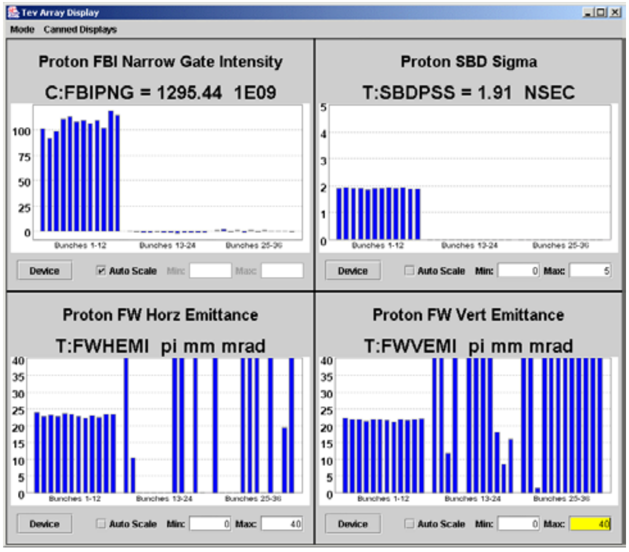

Figure 11: TevArray display with emittances for 12 bunches after the ramp on the proton helix.

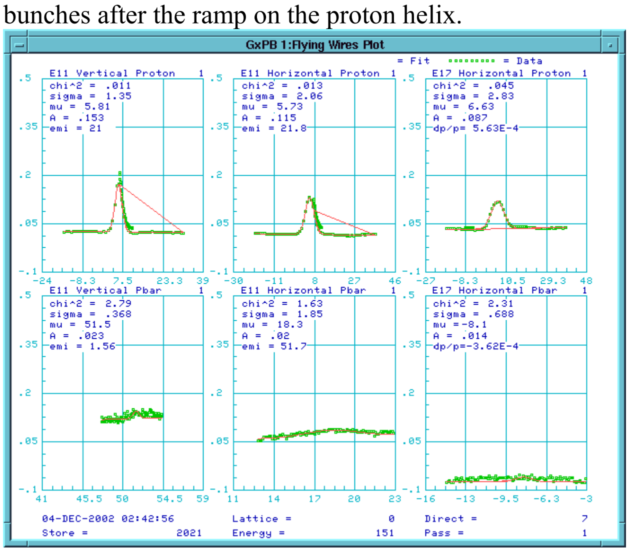

Figure 12: Flying-wires beam profile and the deduced emittance for a single bunch on the central orbit prior to scraping.

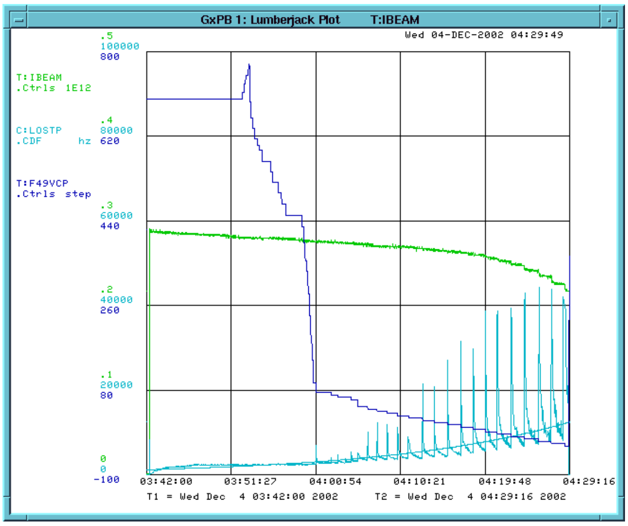

Figure 13: Vertical collimator position, beam intensity, and loss rates during aperture reduction and scraping for a single bunch on the central orbit.

3 RESULTS

The evolution of the proton beam intensity on the proton helix is displayed in Fig. 14, together with the proton loss rate. In the loss rate, many spikes are visible. These correspond to the dry-firing of the pbar injection kickers. The beam lifetime was not visibly affected.

The proton beam lifetime was measured both on the proton and pbar helix. The decay of the beam intensity with time on either helix is displayed in Figs. 15 and 16. The evolution on the proton helix is well described by an exponential fit with lifetime 2.7 hours, which is also shown in Fig. 14. For the antiproton helix, the first few minutes of the decay deviate from an exponential, but can be approximated by a quasi-exponential whose exponent is proportional to the square root of time or by a low-order expansion of such an exponential, as is illustrated in Fig. 15. Part of this difference might be attributed to the different number of bunches (12 versus 1) and hence injection times. Ignoring the short initial steep part of the decay, the fitted lifetime on the pbar helix is roughly the same as that on the proton helix.

We also attempted to fit the lifetime to an inversely linear decay law of the form $N(t)=N(0)/(1+t/\tau_{1/2})$, which is expected, if the decay rate is proportional to the square of the current, i.e., $dN/dt=-\alpha N^2$, from which $\tau=1/(\alpha N(0))$. Fit results to this dependence are compared in Figs. 17 and 18 with those to the exponential or quasi-exponential for the two helices. In these figures we do not observe any qualitative difference between the proton and pbar helix.

Table 1 compiles the fitted beam-current decay times for the three different parametrizations. All the fits were performed over two different time ranges, 15 and 40 minutes. If the decay law is strictly valid, the fitted time constants should be the same for either fit range. Evidently, none of our assumed dependencies fulfils this requirement, and the time constants fitted over 40 minutes are typically two or three times larger than those obtained for the first 15 minutes, i.e., after an initial beam 'shaving' the decay slows downs. The bunch length evolution was also recorded, but only for the proton helix (SBD data were not available when the beam was on the pbar helix). Figure 19 shows an example, along with the fit to an exponential decay. The fitted exponential decay time constant for the bunch length decrease is also listed in Table 1. It is much longer than the current decay time, so that not all of the beam loss can be related to longitudinal shaving.

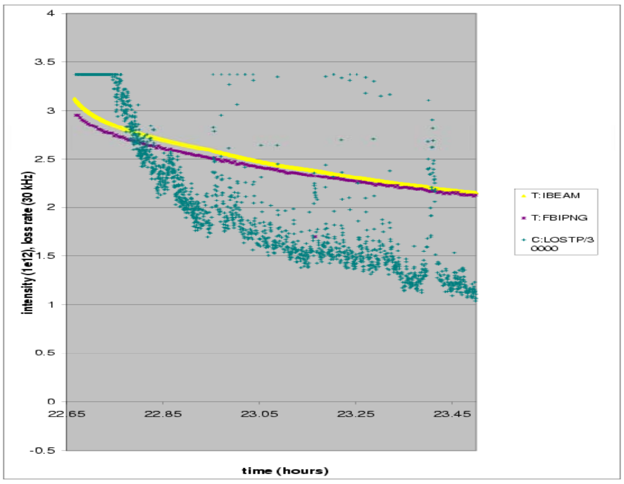

Figure 14: Total intensities T:IBEAM & C:FBIPNG and proton loss rate as a function of time in hours, during a store of 12 proton bunches on the proton helix. The spikes in the loss rate correspond to the dry firing of the pbar injection kickers

.

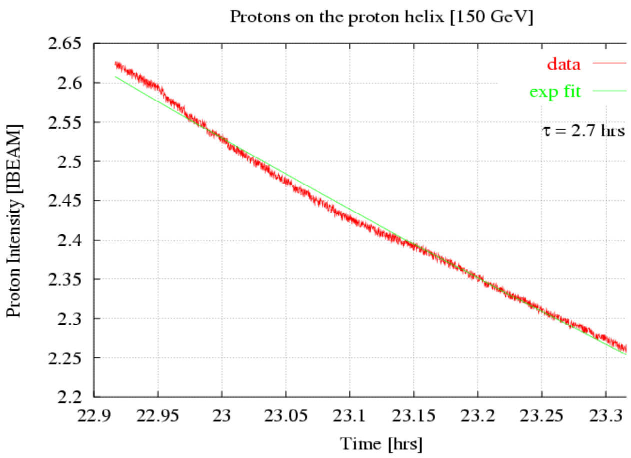

Figure 15: Proton beam intensity as a function of time on the proton helix, and an exponential fit to the data (T. Sen).

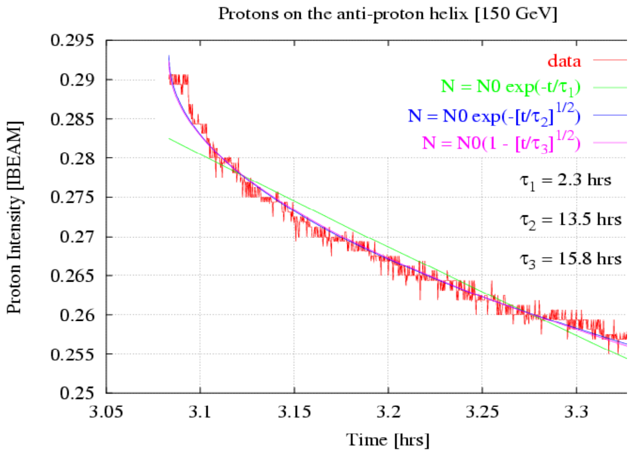

Figure 16: Proton beam intensity as a function of time on the pbar helix, and three different fits to the data (T. Sen).

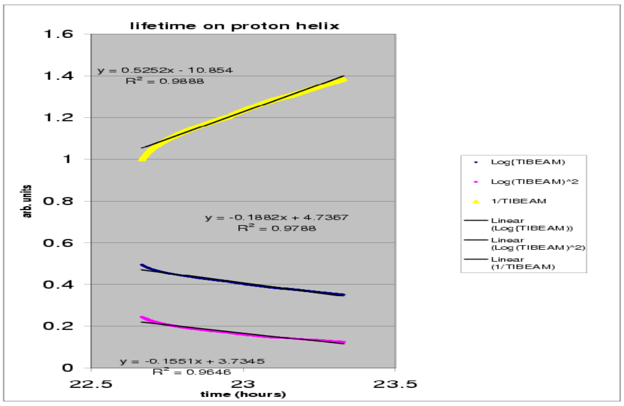

Figure 17: Logarithm of the beam intensity, the square of this logarithm, and the inverse of the beam intensity as a function of time in units of hours, and the linear fits to these three curves, for the proton helix.

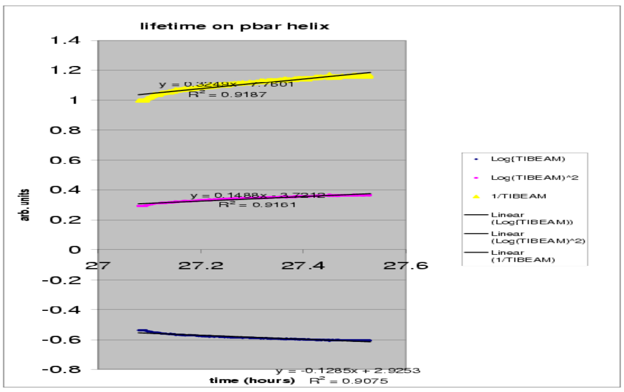

Figure 18: Logarithm of the beam intensity, the square of this logarithm, and the inverse of the beam intensity as a function of time in units of hours, and the linear fits to these three curves, for the antiproton helix.

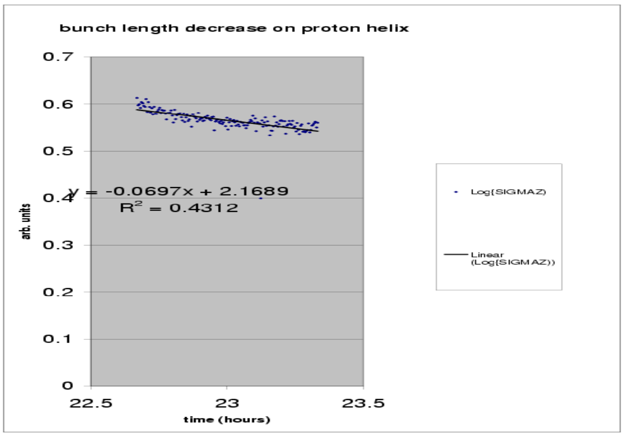

Figure 19: Decrease of the logarithm of the rms bunch length with time, on the proton helix, and a linear fit to the data.

Table 1: Fitted lifetimes for the beam intensity, considering three different models, and exponential decay time for the bunch length, on the two helices.

	model	10 minutes	40 minutes
p helix	exponential	2.5 hr	5.3 hr
	inversely linear	1.0 hr	1.9 hr
	quasi-exponential	2.7 hr	6.4 hr
	bunch length (exp.)	5.4 hr	14.3 hr
pbar helix	exponential	3.1 hr	7.8 hr
	inversely linear	1.3 hr	3.1 hr
	quasi-exponential	2.8 hr	6.7 hr

The proton loss rate was measured on the proton helix as a function of the horizontal and vertical tune, which were varied over a range of roughly +/-0.005 around the nominal working point. Results of the two-dimensional tune scan on the proton helix are illustrated in Figs. 20 and 21, which display the projections of the loss rate onto the horizontal or vertical tune axis. The nominal tune settings are 0.61 and 0.583 (the settings are different from the actual tunes!) The nominal horizontal tune setting coincides with a minimum in the loss rate. It appears that losses can be improved and/or the sensitivity to the horizontal tune be decreased by lowering the vertical tune setting by about 0.004 from our nominal starting point. This would bring the tunes closer to the diagonal.

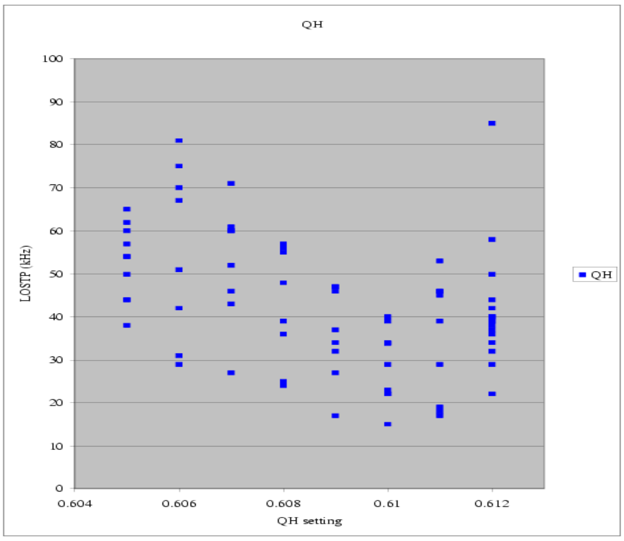

Figure 20: Projection of the measured proton loss rate onto the horizontal tune axis, for the two-dimensional tune scan on the proton helix.

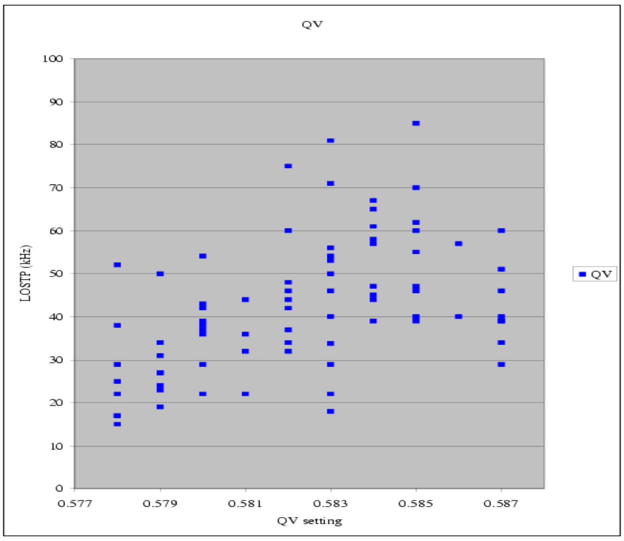

Figure 21: Projection of the measured proton loss rate onto the vertical tune axis, for the two-dimensional tune scan on the proton helix.

The result of the chromaticity scan on the proton helix is shown, in Fig. 22, as the projections of the loss rate onto the two chromaticity axes (here combined in one plot), and, in Fig. 23, as a three-dimensional picture. The initial nominal chromaticity settings were 30 and 43. We see that the loss rate steeply increases, when the chromaticity is raised by 1 or 2 units in either plane. The chromaticity scan on the pbar helix is illustrated in Fig. 24. In this case the initial chromaticity settings were 32 and 42, om ythe rising edge of the loss rates. Note that the scan on the pbar helix was performed with a single bunch, the scan on the proton helix with 12 bunches. When comparing the absolute values of the loss rates we should thus multiply the pbar-helix values by 12, and find that the loss rates on the pbar helix stay well below those on the proton helix. This might explain the presently much better lifetime of the pbars as compared with the protons at injection. At the setting Ch=42, Cv=29 on the pbar helix a sudden instability occurred, by which we lost two thirds of the beam current. Note that we could drop the chromaticity much further on the proton helix (with 12 bunches instead of 1), without ever encountering an instability threshold. This difference between the two helices might be another possible reason why during an earlier experiment at 980 GeV [1] the pbars, but not the protons, became unstable when we dropped the two chromaticities. (The chromaticity differential induced by the long-range beam-beam collisions was put forward as an explanation for that other study, but in the present experiment, at 150 GeV, there was only 1 beam, and still a clear difference between the two helices could be noted.)

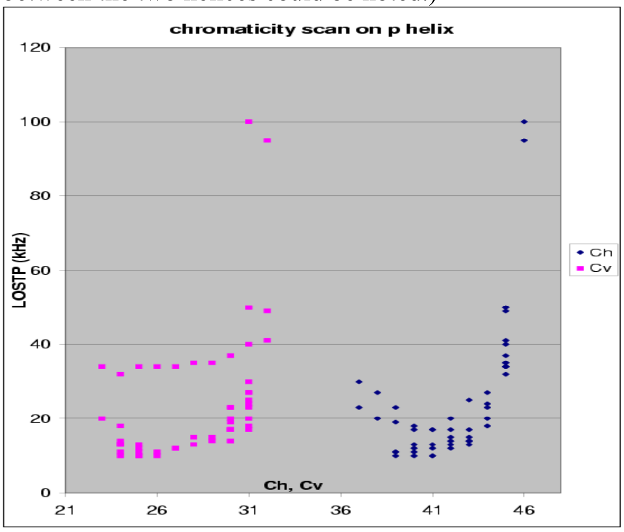

Figure 22: Projection of the measured proton loss rate for 12 bunches on the two chromaticity axes, for the two-dimensional scan of chromaticities on the proton helix. the beam due to an instability.

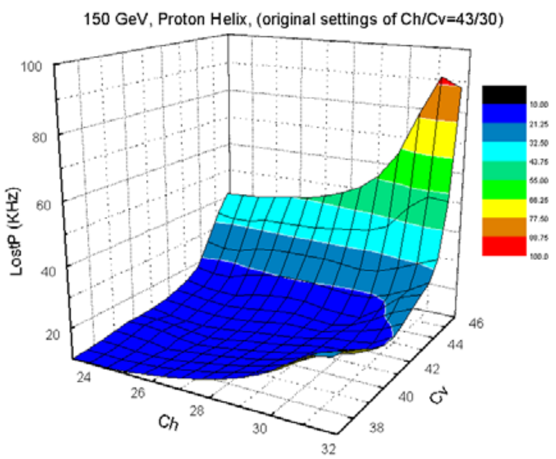

Figure 23: Proton loss rates for 12 bunches on the proton helix vs. horizontal & vertical tune (X.L. Zhang).

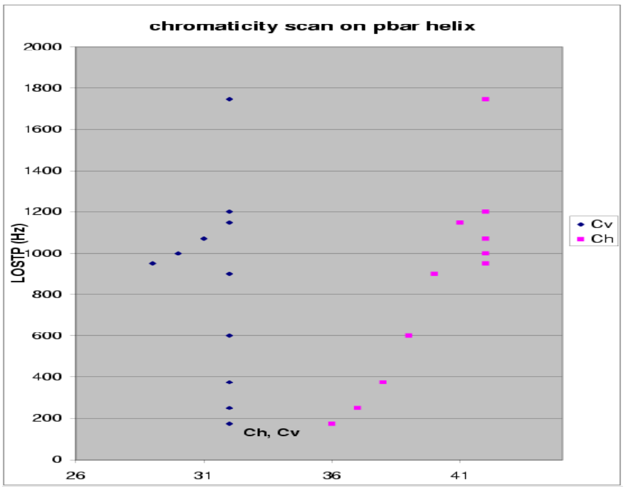

Figure 24: Projection of the measured proton loss rate for a single bunch on the two chromaticity axes, for the two-dimensional scan of chromaticities on the pbar helix. At Ch=42, Cv=29, we lost two thirds of the beam due to an instability.

The calibration of the tune knobs on the central orbit is depicted in Figs. 25 and 26. The slopes are within 15-25% of the expected values, but there is a significant non-orthogonal component (change in the other tune) of 10-30%. The tune-knob calibration is summarized in Table 2. Part of the discrepancy might be attributed to coupling.

Table 2: Tune knob calibration on the central orbit at 150 GeV. The linear dependence (slope) of the measured tunes on the knob settings is shown; deviations from 1 and 0 indicate a calibration error or non-orthogonality, respectively.

	meas. QX slope	meas. QY slope
QX knob	0.94	0.29
QY knob	0.13	0.76

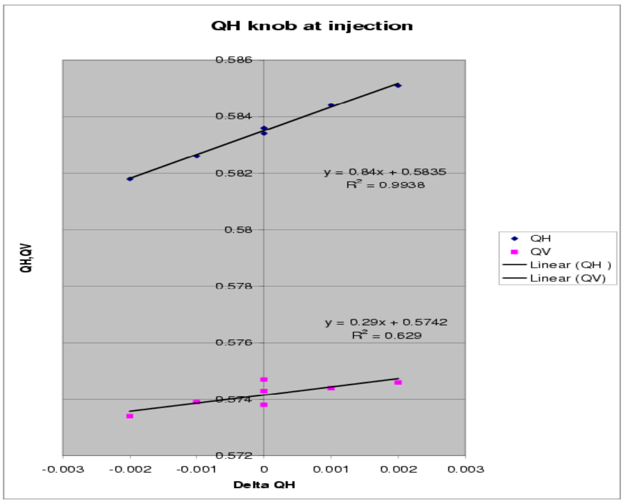

Figure 25: Calibration of the horizontal tune knob on the proton helix. The measured horizontal and vertical tunes are plotted against the horizontal tune-knob change.

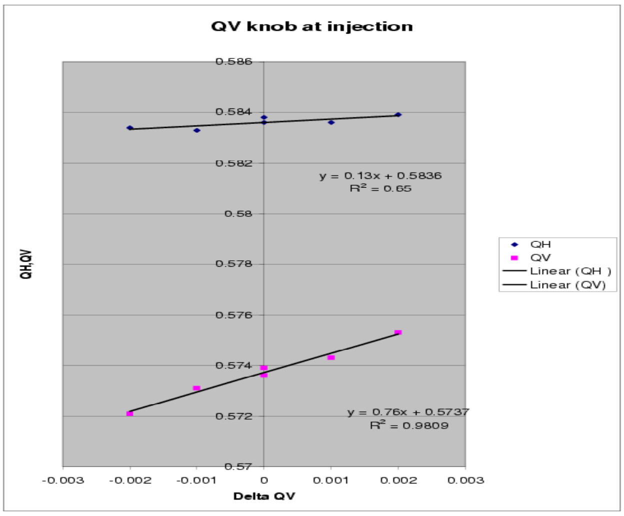

Figure 26: Calibration of the vertical tune knob on the proton helix. The measured horizontal and vertical tunes are plotted against the horizontal tune-knob change.

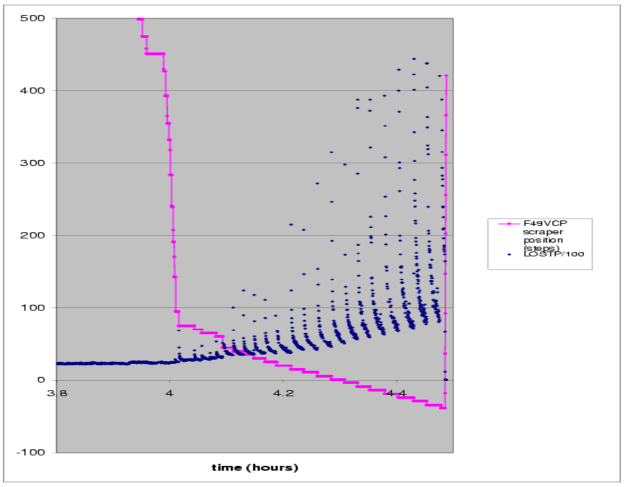

Figure 27: Collimator position in units of steps (1 step = 1 mil) and proton loss rate (in units of 100 Hz) as a function of time in hours during the proton scraping experiment.

Figure 27 shows the change of loss rates and collimator position during the scraping experiment for a single bunch on the central orbit. The collimator moved inwards by almost 2 cm, before the loss rate noticeably increased. Then, at each further step of the collimator, the losses went up steeply and then gradually decreased. Since we were removing part of the beam the loss rate is not directly related to the steady-state beam lifetime at each aperture. We made an attempt to estimate the variation of the latter from the minima of the loss rate just prior to each new step. This is perhaps legitimate, since the since the time interval between steps was approximately constant. We than obtain a relation between the 'steady' loss and the collimator position, which is displayed in Fig. 28. If the collimator is far away from the beam, the losses are approximately constant. At a step position of about +100 the losses start to increase steeply towards smaller collimator positions. Linear and exponential fits to the variable and constant part of the curve are included in the plot. The exponential fit describes the dependence of the loss rate on the aperture extremely well. Assuming that the 'steady' loss rate is inversely proportional to the beam lifetime, an exponential dependence of the lifetime on the aperture a is expected, namely

$$\tau \propto \exp\left(\frac{a}{a_0}\right),$$

where the numerical value of the constant a_0 is deduced from the fit in Fig. 29. It is about 2.5 mm at the location of the collimator, or 2.5 times the rms beam size (assuming β_y=43 m and a $6\sigma^2$ normalized emittance of 20 μm).

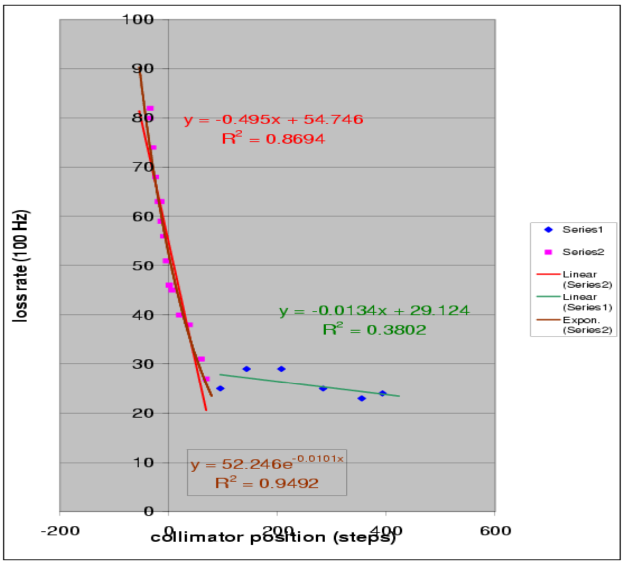

Figure 28: Loss rate prior to a collimator step versus the collimator position. Linear and exponential fits to the two parts of the curve are superimposed.

Figure 29 displays the change in beam current during the scraping experiment, together with the collimator position on an expanded scale. About 20% of the protons were removed by the single collimator, before the beam was dumped. As in earlier studies [2,3] we tried to fit the measured beam loss as a function of collimator position, in order to determine the beam size at the collimator. The fit result is displayed in Fig. 30. The coefficient of the quadratic component is $-(1/(2\sigma^2))$ [2,3]. The fit yields an rms beam size σ=1.8 mm. Using β=43 m at collimator F49V, this would correspond to a $6\sigma^2$ normalized emittance of 72 μm. At this time the flying wires reported an emittance of 21 μm (see Fig. 12). Hence, there is a huge discrepancy, which presumably reflects the error of the fit. The accuracy could be much improved by scraping the entire beam.

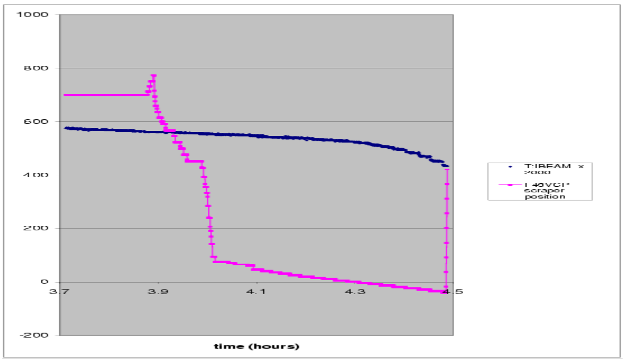

Figure 29: Collimator position in units of steps (1 step = 1 mil) and proton bunch intensity as a function of time in hours, during the proton scraping experiment.

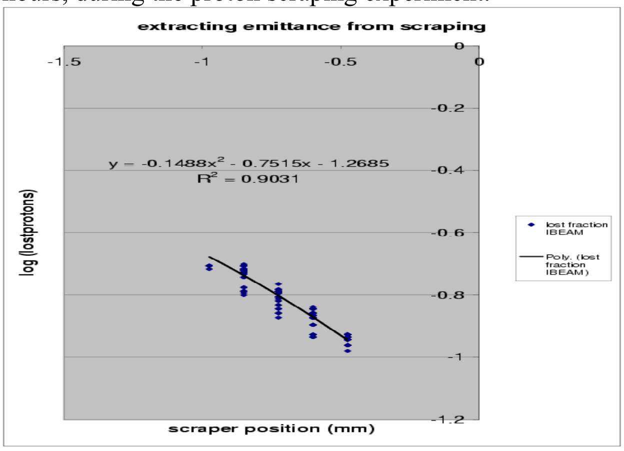

Figure 30: Natural logarithm of the lost fraction of protons as a function of scraper position, and a parabolic fit to the data. The three fit coefficients yield the centre position of the beam and the beam size at the collimator. The last coefficient can be used to verify that the fit is consistent with the model assumption.

4 CONCLUSIONS

The differential chromaticities between proton helix and pbar helix at 150 GeV are about 3 or 4 units (chromaticities on the pbar helix being lower). We calibrated the tune control knobs in T55, also at 150 GeV, and found that these are 'almost' correct. The scaling is within 15-30% from 1 and, in addition, there is a non-orthogonality of 10-30%. The scaling seemed to vary with the tune, which is most likely due to coupling. The exponential lifetime of a nominal coalesced bunch is about 2.5 hours, as fitted over 15 minutes on either helical orbit, perhaps marginally higher for the pbar helix. We have attempted alternative fits to the beam lifetime considering various semi-empirical decay laws, and found that none of them correctly describes the intensity decrease over 40 minutes, though one can improve on a purely exponential fit. On the proton helix, the beam lifetime and loss rates are quite sensitive to the tunes. The nominal tunes are not far from the optimum, but a reduction by –0.002 or –0.004 in the vertical tune might make the lifetime a bit better and also further desensitize the working point. On the proton helix losses, the loss rates show a threshold value for both chromaticities, above which the proton losses quickly become unbearable. In particular, the loss rate is not simply proportional to the chromaticity. For lower values, there is a broad plateau with little sensitivity. The nominal chromaticity is about 2 or 3 units below the threshold in the loss rate. We observed a vertical instability on the pbar helix when the vertical chromaticity wsa dropped by about 3-4 units, and 75% of the beam was lost. No such instability was seen on the proton helix, where the chromaticities were scanned over a much wider range. This can be explained partly, but not entirely, by the chromaticity differential between the two helices. As expected, we observed that the beam lifetime becomes worse, if a hard aperture (collimator) is closer to the beam. The loss-rate data indicate an exponential dependence on the aperture, with an e-folding coefficient equal to 2.5 times the rms beam size. Finally, the vertical emittance deduced from the scraping is a factor 3-4 higher than the emittance reported from the flying wire (by contrast, in two previous studies at 980 GeV, the emittance inferred from scraping was 2 times lower than the flying-wire emittance [2,3]).

5 ACKNOWLEDGEMENTS

We thank the Tevatron operations crew for the friendly and reliable assistance.

REFERENCES

[1] X.L. Zhang, F. Zimmermann, 'Tevatron Study Report: Losses vs. Chromaticity 11/26/02'.
[2] V. Shiltsev, X.L. Zhang, F. Zimmermann, 'Tevatron Study report: Pbar Tunes & Pbar removal 11/17/02'.
[3] J. Annala, V. Shiltsev, D. Still, C.Y. Tan, X.L. Zhang, F. Zimmermann: 'Tevatron Study Report: Measuring Pbar Tunes with Tan's System, Beam Separation, and Pbar Removal 12/03/02'.